NASA Contractor Report 3321

Satellite Power Systems (SPS) Concept Definition Study

Volume IV - Transportation Analysis

G. M. Hanley
Rockwell International
Downey, California

Prepared for
Marshall Space Flight Center
under Contract NAS8-32475

National Aeronautics
and Space Administration

**Scientific and Technical
Information Branch**

1980

APPENDIX A

HORIZONTAL TAKEOFF - SINGLE STAGE TO ORBIT TECHNICAL SUMMARY

A.0 INTRODUCTION

Evolving Satellite Power System (SPS) program concepts envision the assembly and operation of sixty solar-powered satellites in synchronous equatorial orbit over a period of thirty years. With each satellite weighing approximately 35 million kiolgrams, economic feasibility of the SPS is strongly dependent upon low-cost transportation of SPS elements. The rate of delivery of SPS elements alone to LEO for this projected program is 70 million kilograms per year. This translates into 770 flights per year or 2.1 flights per day using a fleet of vehicles, each delivering a cargo of 91,000 kilograms.

The magnitude and sustained nature of this advanced space transportation program concept require long-term routine operations somewhat analogous to commercial airline/airfreight operations. Vertical-takeoff, heavy lift launch vehicles (e.g., 400,000 kg payload) can reduce the launch rate to 175 or more flights per year. However, requirements such as water recovery of stages with subsequent refurbishment, stacking, launch pad usage, and short turnaround schedules introduce severe problems for routine operations. Studies performed previously showed that substantial operational advantages are offered by an advanced horizontal takeoff, single-stage-to-orbit (HTO-SSTO) aerospace vehicle concept. Further analysis of this concept was needed to provide a promising alternative to vertical launch heavy lift launch vehicle approaches for LEO logistics support of the SPS.

The technical problems requiring investigation were of two types: (a) the need for further development of the vehicle system concept including a multicell wet wing containing cryogenic propellants in a blended wing-body configuration; and (b) technology issues, particularly the technical feasibility and performance potential of an advanced hybrid airbreathing engine system, and technical assessment of a flight mode involving horizontal takeoff, long range cruise, subsequent insertion into an equatorial orbit and return via aeromaneuver to the higher-latitude take-off site.

The general objective of this study was to improve system definition and to advance subsystem technologies for a horizontal takeoff, single-stage-to-orbit vehicle which can provide economical, routine earth-to-LEO transportation in support of the Satellite Power Systems program. Specific objectives were:

1. To improve the design definition and technical and operational features of the HTO-SSTO vehicle concept primarily using existing aerodynamic, aerothermal, structural, thermal protection, airbreather and rocket propulsion, flight mechanics and operations technology integrated into a total systems design.

2. To identify disciplines and subsystems in which the application of advanced technology would produce the greatest increase in system performance, and to advance technologies in specific areas.

The primary elements of the HTO-SSTO study and the related technology issues are summarized in Figure A-1. Technical briefings and study progress briefings were given to NASA Headquarters, MSFC, JSC and LaRC, and to USAF/SAMSO. A code showing the general level of technical assurance of the study data as being suitable for feasibility confirmation is placed adjacent to technology items. A filled square, ■ , indicates a high degree of confidence in analytical methods and results. A half-filled square, ◪ , indicates data requiring further technical analyses. The hollow square, □ , relates to technology issues not analyzed or which will require detailed in-depth analysis to produce data suitable for feasibility confirmation.

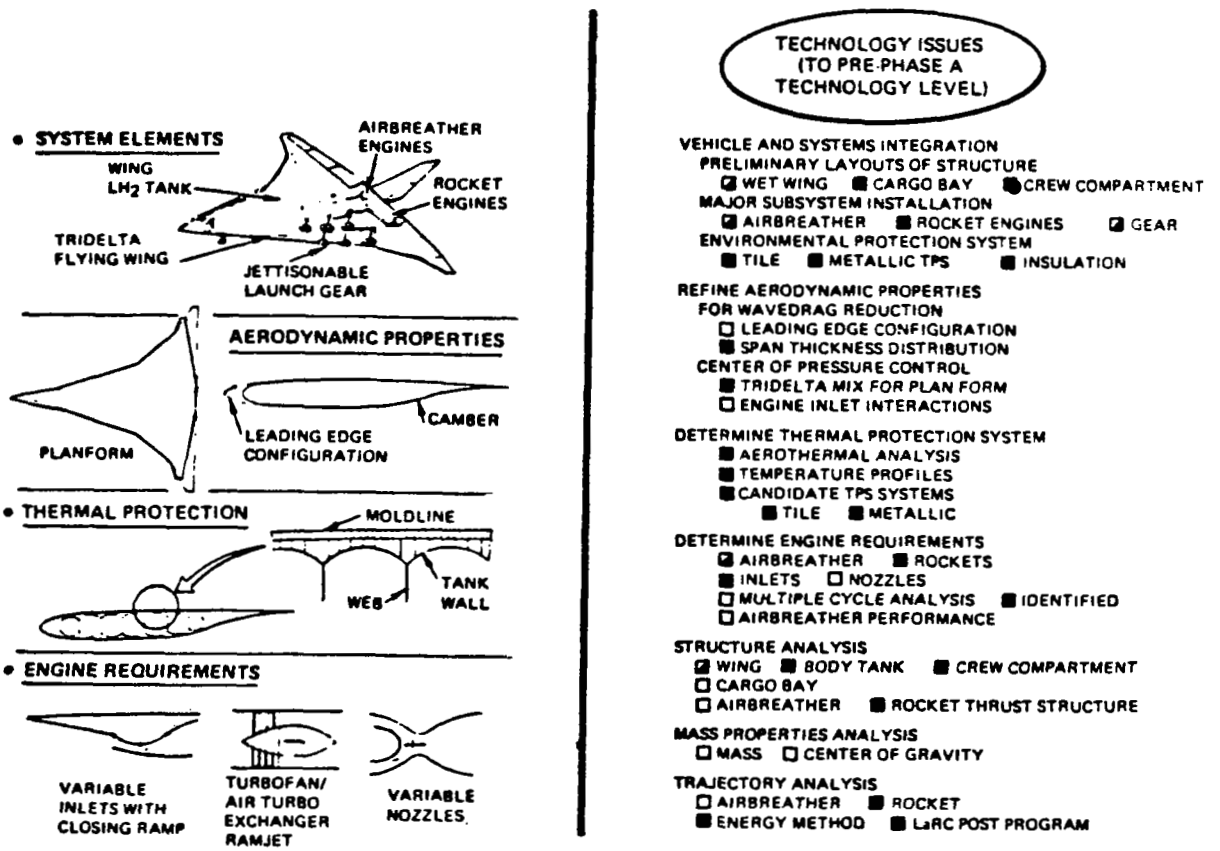

Figure A-1. Study Summary -- Advanced Transportation System for SPS

The combined systems design/performance and technology development studies produced a number of significant results.

1. Demonstrated, with end-to-end simulation, the ability of the vehicle to take off from KSC, cruise to the equatorial plane, insert into a 300 nmi equatorial orbit with 151,000-pound payload, and then to re-enter and return to the launch site; also to deliver a 196,000-pound payload with a due-East launch.

2. Devised a modified airbreathing engine cycle for operation in turbofan, air-turbo-exchanger and ramjet modes to provide an effective match with takeoff, cruise and acceleration requirements.

3. Showed that the HTO-SSTO lower surface temperatures during reentry are several hundred degrees lower than the STS orbiter lower surface temperatures because of a lower wing loading. As a result, an advanced titanium aluminide system shows promise of being lighter than the RSI tile for this application.

This study was funded primarily by Rockwell IR&D funds and a summary only is contained herein.

A.1 OPERATIONAL FEATURES

The HTO-SSTO concept adapts existing and advanced commercial and/or military air transport system concepts, operations methods, maintenance procedures, and cargo handling equipment to include a space-related environment. The principal operational objective is to provide economic, reliable transportation of large quantities of material between earth and LEO at high flight frequencies with routine logistics operations and minimal environmental impact. An associated operational objective was to reduce the number of operations required to transport material and equipment from their place of manufacture on earth to low earth orbit.

Operations features derived in the study are as follows:

- Single orbit up/down to/from the same launch site (at any launch azimuth subject to payload/launch azimuth match)

- Capable of obtaining 300 nmi equatorial orbit when launched from KSC

- Takeoff and land on 8,000 to 14,000-foot runways (launch velocity $\approx$ 225 knots; landing velocity $\leq$ 115 knots)

- Simultaneous multiple launch capability

- Total system recovery including the takeoff gear which is jettisoned and recovered at the launch site

- Aerodynamic flight capability from payload manufacturing site to launch site, addition of launch gear and fueling, and launch into earth orbit

- Amenable to alternative launch/landing sites
- Incorporates Air Force (C-5A Galaxy) and commercial (747 cargo) payload handling, including railroad, truck, and cargo-ship containerization concepts, modified to meet space environment requirements
- Swing-nose loading/unloading, permitting normal aircraft loading-door facility concept application
- Propulsion system service using existing support equipment on runway aprons or near service hangars
- In-flight refueling options (option not included in reference vehicle data)

A.2 DESIGN FEATURES

The HTO-SSTO utilizes a tri-delta flying wing concept, consisting of a multi-cell pressure vessel of tapered, intersecting cones. The tri-delta planform (blended fuselage-wing) and a Whitcomb airfoil section offer an efficient aerodynamic shape from a performance standpoint and high propellant volumetric efficiency. The outer panels of the wing and vent system lines in the wing's leading edge provide the gaseous ullage space for LH_2 fuel. LH_2 and LO_2 tanks are located in each wing near the vehicle, c.g., and extend from the root rib to the wing tip LH_2 ullage tank (Figure A-2). Approximately 20% of the volume of the vertical stabilizer is utilized as part of the gaseous ullage volume of the integral wing-mounted LO_2 tanks. In the aft end of the vehicle, three uprated high-P_c rocket engines (thrust = 3.2×10^6 lb) are attached with a double-cone thrust structure to a two-cell LH_2 tank.

Most of the cargo bay side walls are provided by the root-rib bulkhead of the LH_2 wing tank. The cargo bay floor is designed similar to the C5-A military transport aircraft. This permits the use of MATS and Airlog cargo loading and retention systems. The top of the cargo bay is a mold-line extension of the wing upper contours, wherein the frame inner caps are arched to resist pressure at minimum weight. The forward end of the cargo bay has a circular seal/docking provision to the forebody. Cargo is deployed in orbit by swinging the forebody to 90 or more degrees about a vertical axis at the side of the seal, and transferring cargo from the bay into space or to in-space receivers on telescoping rails.

The forebody is an RM-10 ogive of revolution with an aft dome closure. The ogive is divided horizontally into two levels. The upper level provides seating for crew and passengers, as well as the flight deck. The lower compartment contains electronic, life support, power (fuel cell), and other subsystems including spare life support and emergency recovery equipment.

Ten high-bypass, supersonic-turbofan/airturbo-exchanger/ramjet engines with a combined static thrust of 1.4×10^6 lb are mounted under the wing. The inlets are variable area retractable ramps that also close and fair the bottom into a smooth surface during rocket powered flight and for high angle-of-attach ballistic re-entry.

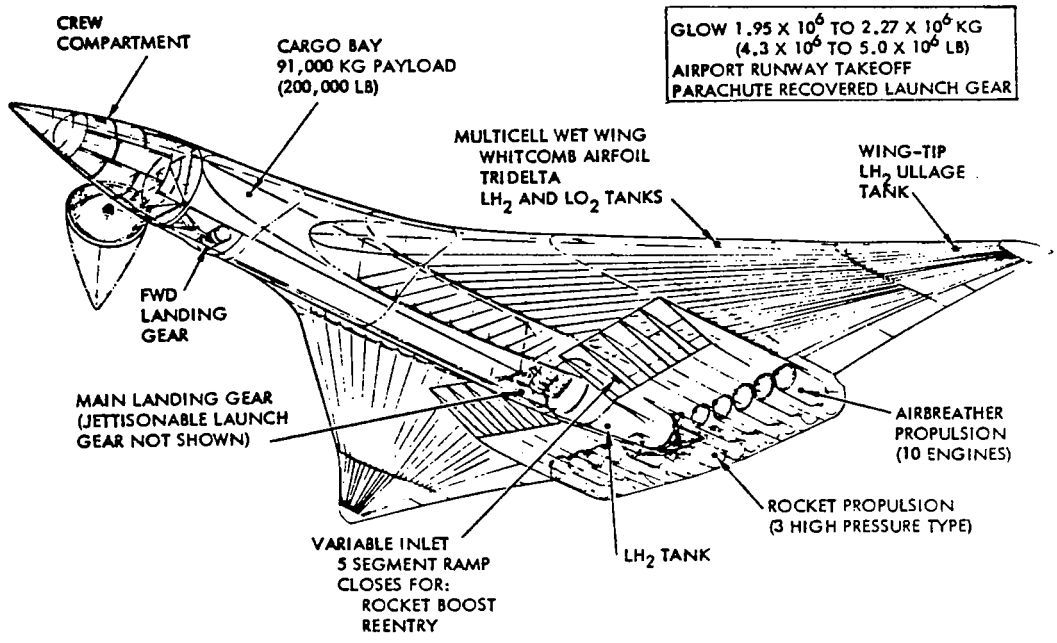

Figure A-2. HTO-SSTO Design Features

Figure A-3 shows an inboard profile of the vehicle, illustrating the details of body construction, crew compartment, cargo bay length, LH_2 tank configuration, and location of the rocket engines at rear of fuselage. The hinging and rotation of the nose section for loading and unloading the payloads are illustrated, with indication of view angle from the rear of the nose section during these operations. The multiple landing gear concept shows the position of the nose gear bogie, the jettisonable takeoff gear, and the main landing gear for powered landing.

Figure A-4 presents front and rear views of the vehicle showing the blended wing, engine inlet ducts, landing gear arrangement, and vertical stabilizer. Also shown are typical sections through the vehicle at:

- The hinge line section (B-B) aft of the crew compartment and forward of the nose gear. Cross-sectional dimensions of the cargo bay are indicated.
- The 40% chord line fuselage section (C-C) illustrating the wing and fuselage construction and the profile of the wing/fuselage fairing.
- The main landing gear station (D-D) illustrating the gear retraction geometry, the relationship of the gear to the engine air inlet ducts and the wing construction and profile to the fuselage shape.

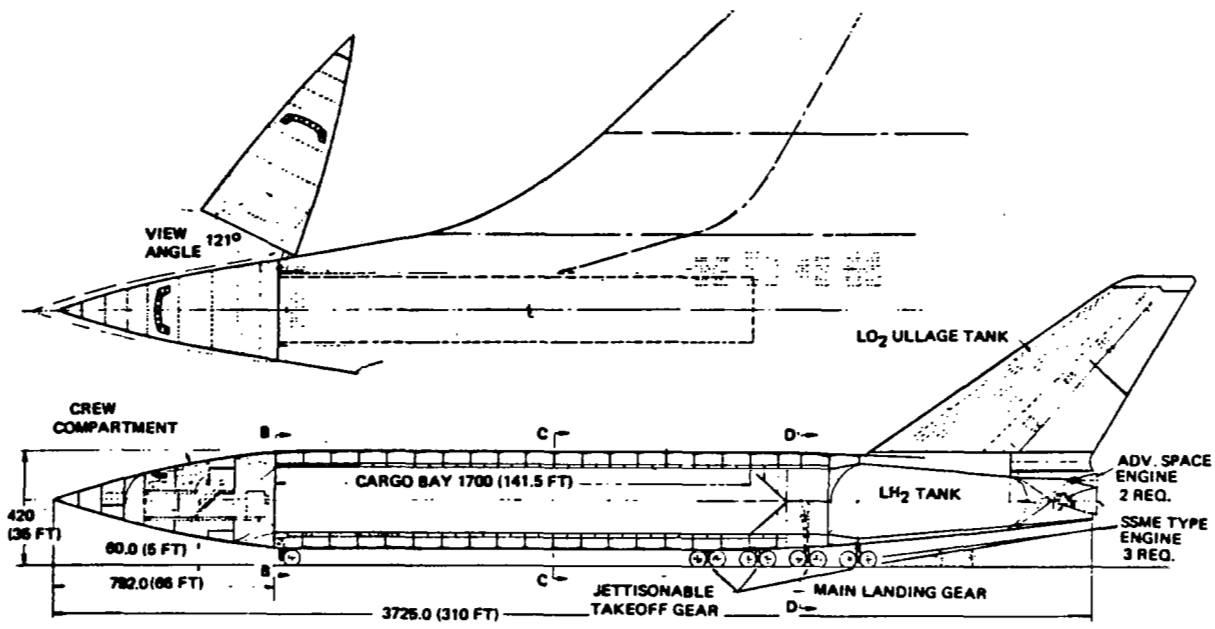

Figure A-3. HTO-SSTO Inboard Profile

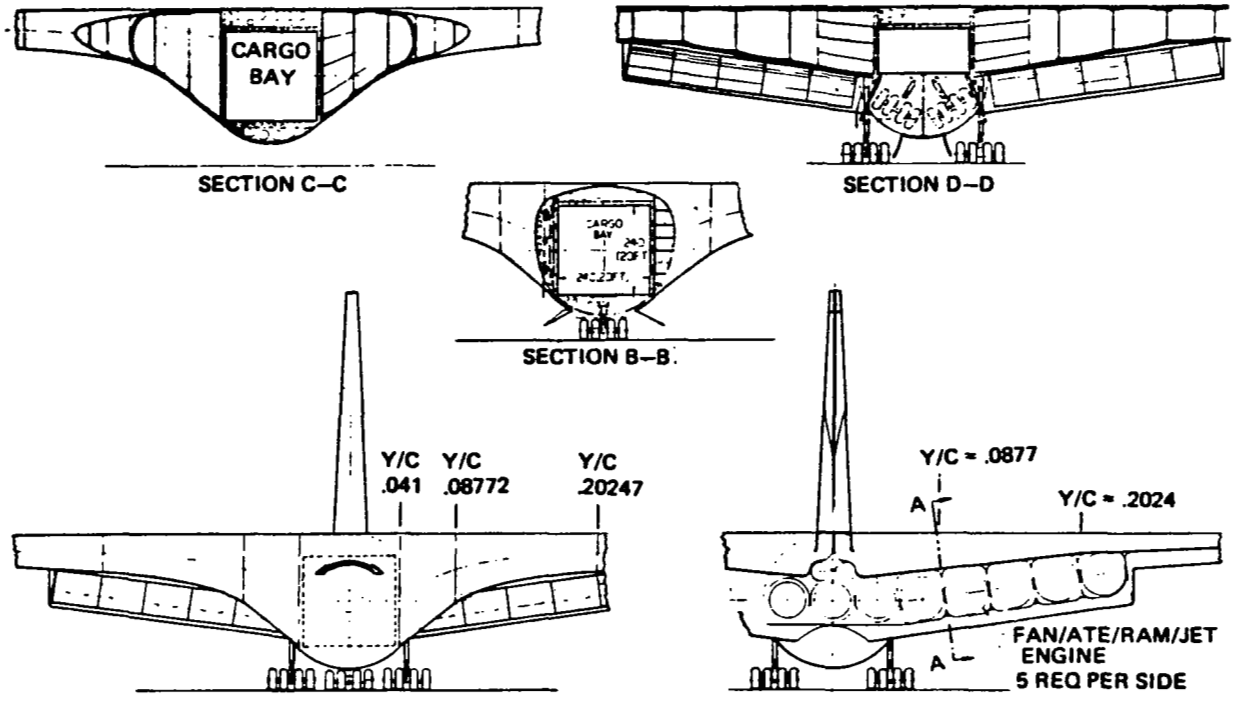

Figure A-4. Vehicle Section Results

Figure A-5 presents details of the basic multi-cell structure of the wing. The upper portion illustrates the application of "Shuttle-type" RSI tile thermal protection system (TPS). The lower portion shows a potential utilization of a "metallic" TPS.

The wing is an integrated structural system consisting of an inner multi-cell pressure vessel, a foam-filled structural core, an inner facing sheet, a perforated structural honeycomb core, and an outer facing sheet. The inner multi-cell pressure vessel arched shell and webs are configured to resist pressure. The pressure vessel and the two facing sheets, which are structurally interconnected with phenolic-impregnated, glass fiber, honeycomb core, resist wing spanwise and chordwise bending moments. Cell webs react winglift shear forces. Torsion is reacted by the pressure vessel and the two facing sheets as a multi-box wing structure.

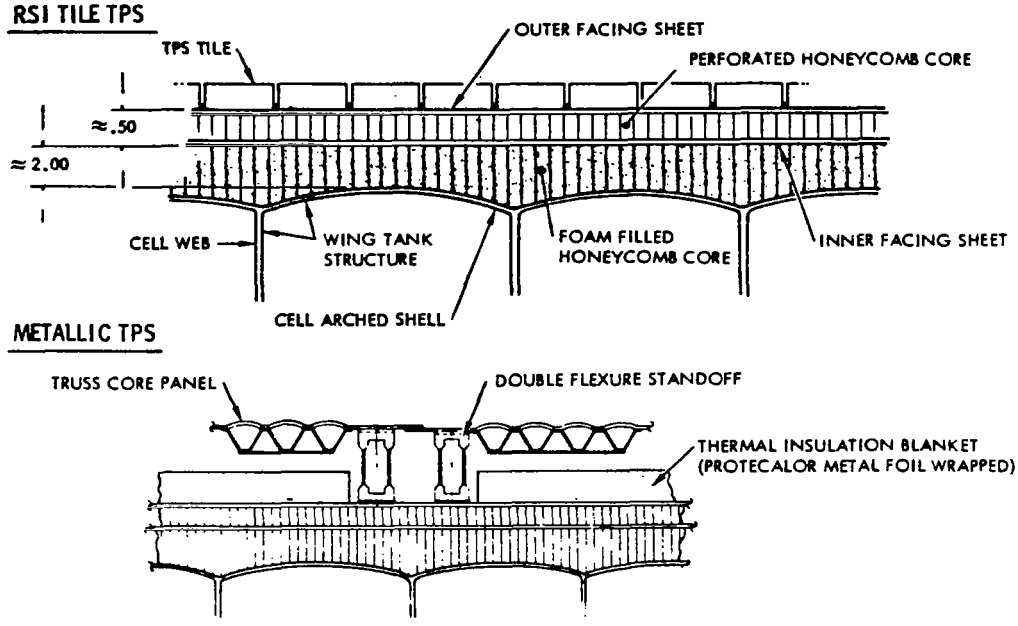

Figure A-5. Wing Construction Detail with Candidate TPS Configurations

The outer honeycomb core is perforated and partitioned to provide a controlled passage, purge and gas leak detection system function in addition to the function of structural interconnect of the inner and outer facing sheets. The construction of the wing structure utilizes the "Inflation Assembly Technique" developed by Rockwell for the Saturn II booster common bulkhead.

A.3 MULTI-CYCLE AIRBREATHER ENGINE SYSTEM

Takeoff and climb to 100,000 ft altitude and 5,800 fps is by airbreather propulsion. Parallel burn of airbreather and rocket propulsion occurs between 5,800 to 7,200 fps. Rocket power is then employed from 7,200 fps to orbit.

The multi-cycle airbreathing engine system, Figure A-6 is derived from the General Electric CJ805 aircraft engine, the Pratt and Whitney SWAT 201 supersonic wrap-around turbofan/ramjet engine, the Aerojet Air Turborocket, Marquardt variable plug-nozzle, ramjet engine technology, and Rocketdyne tubular-cooled, high-P_C rocket engine technology.

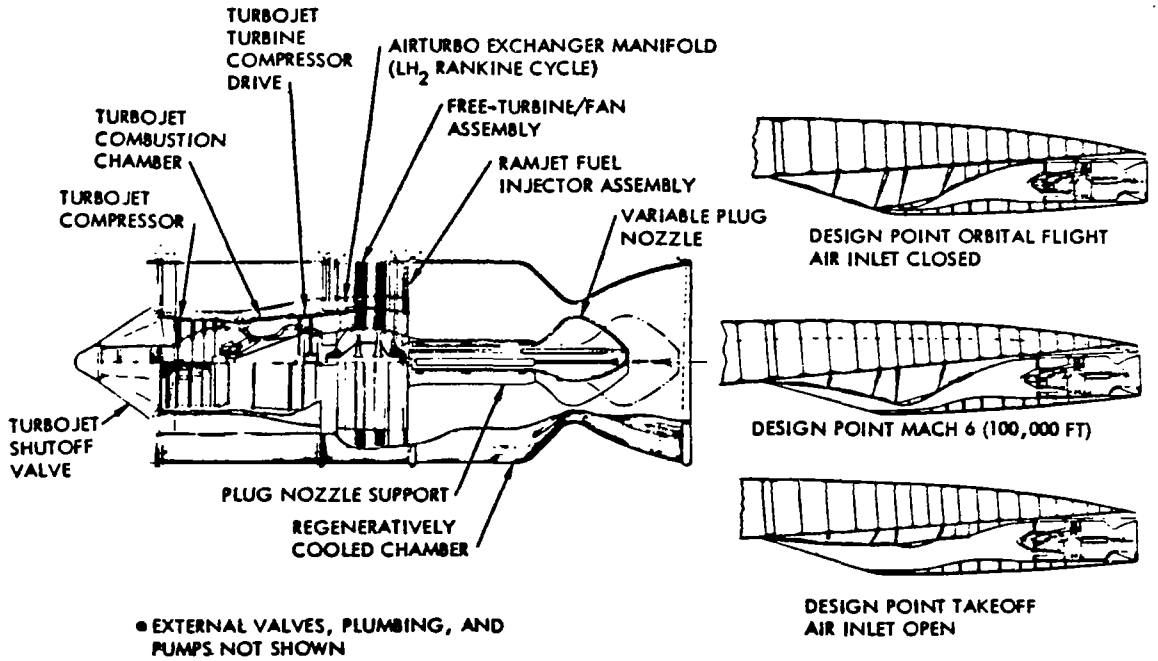

Figure A-6. Multi-Cycle Airbreathing Engine and Inlet, Turbofan/Air Turboexchanger/Ramjet

The multi-mode power cycles include: an aft-fan, turbofan cycle, a LH_2, regenerative Rankine, air-turboexchanger cycle; and a ramjet cycle that can also be used as a full flow (turbojet core and fan bypass flow) thrust-augmented turbofan cycle. These four thermal cycles may receive fuel in any combination permitting high engine performance over a flight profile from sea level takeoff to Mach 6 at 100,000 ft altitude.

The engine air inlet and duct system is based on a five-ramp variable inlet system with actuators to provide ramp movement from fully closed (upper RH figure) for rocket-powered and re-entry flight, to fully open (lower RH figure) for takeoff operation.

The inlet area was determined by the engine airflow required at the Mach 6 design point. The configuration required 1.4×10^6 pounds thrust at the Mach 6 condition and at least 1.2×10^6 pounds for takeoff. This resulted in an inlet area of approximately 1200 ft^2 or 120 ft^2/engine for a 10-engine configuration. In order to provide pressure recovery with minimum spillage drag over the wide range of Mach numbers, a variable multi-ramp inlet is required. Inlet pressure recovery efficiency vs. velocity is plotted on Figure A-7. Higher recoveries are possible for the HTO vehicle than for military aircraft which must operate

during more violent maneuvers. However, the pressure recovery must still provide a margin which prevents inlet instability and possible engine flameout from expulsion of the normal shock during transients.

Estimated engine thrust (total of 10 engines) versus velocity is given in Figure A-8. Initially, a constant thrust of 1.4 million pounds of thrust was assumed for the Rockwell modified Rutowski energy method trajectory analysis (dashed curve of Figure A-8). A tentative airbreather engine performance map was estimated from engine data sources previously described. Subsequent analyses produced the engine thrust versus Mach number estimate shown by the upper solid curve of Figure A-8.

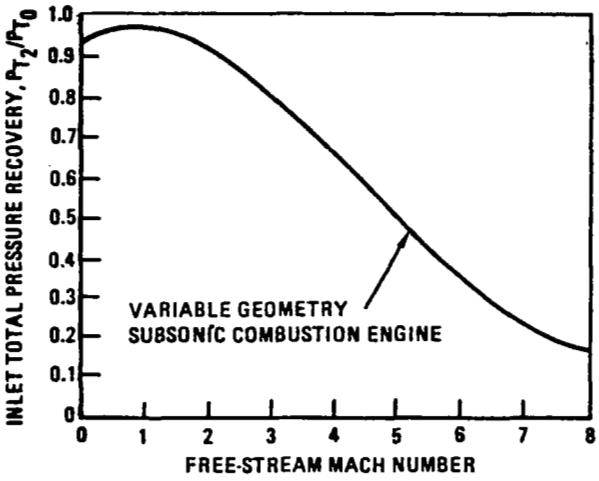

Figure A-7. Air Induction System Performance

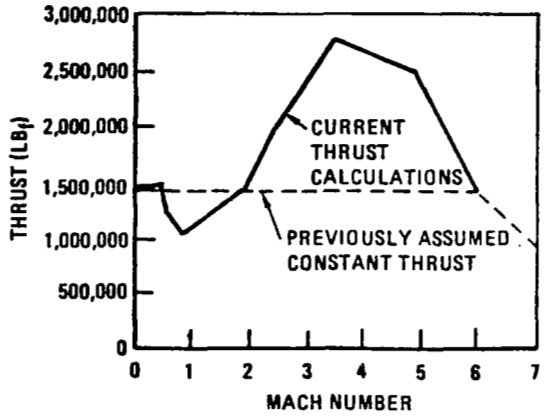

Figure A-8. Airbreather Thrust Versus Mach Number

Major engine companies were contacted to obtain assistance in advanced cycle analysis and to obtain the results of any studies which investigated this operating regime. Data from a Pratt and Whitney report (Reference 1) on an advanced hydrogen burning engine, the SWAT 201 turbofan ramjet, were evaluated and scaled up to the size required. However, this engine, which uses a bypass valve to close off the engine core above Mach 3.1 and operates the afterburner as a ramjet at higher speeds, did not provide a good match of thrust requirements over the required operating range. Also because of the high compression-ratio design, the engine thrust-to-weight ratio (T/W) was in the range of 4.5 to 5.5 for an installed system. Single-stage-to-orbit launch vehicle analysis showed that a T/W of at least 8 would be necessary to meet the vehicle payload requirements. From Aerojet, (Reference 2) data were obtained on an air turborocket concept which provides a potential for meeting the required T/W values while providing a better match of thrust required at takeoff, transonic and supersonic conditions. A modification of this cycle was devised by Rockwell to best match the SSTO requirements. This engine operates as an augmented turbofan for takeoff, a turbofan for high-efficiency cruise, an augmented turbofan for acceleration, and as a ramjet above Mach 3.

The engine components include a rotary vane assembly to close off the compressor-turbine assembly at higher Mach numbers. The use of LH_2 fuel permits the use of a Rankine-cycle air turboexchanger concept to provide power for the bypass fan. This allows elimination of approximately one-half of the normal turbofan compressor stages normally needed for fan drive. Heating of the LH_2 in outer walls and nozzle plug of tubular construction, in addition to providing fan drive power, permits stoichiometric combustion in the augmentor/ramjet by cooling of exposed surfaces. The 5500-degree combustion temperature provides high cycle efficiency. During ramjet mode operation, the fan is allowed to windmill and is cooled by flow of LH_2 through the fan guide vanes.

The scope of this study did not permit a detailed evaluation of engine components to provide further, more accurate calculation of the performance capability of this engine concept. Engine manufacturers are best equipped to further refine the design and provide real data on concept feasibility and system weight.

For preliminary estimation of airbreathing propulsion system size requirement, a computer program was developed for the Hewlett Packard computer. A flow diagram of this program is shown in Figure A-9.

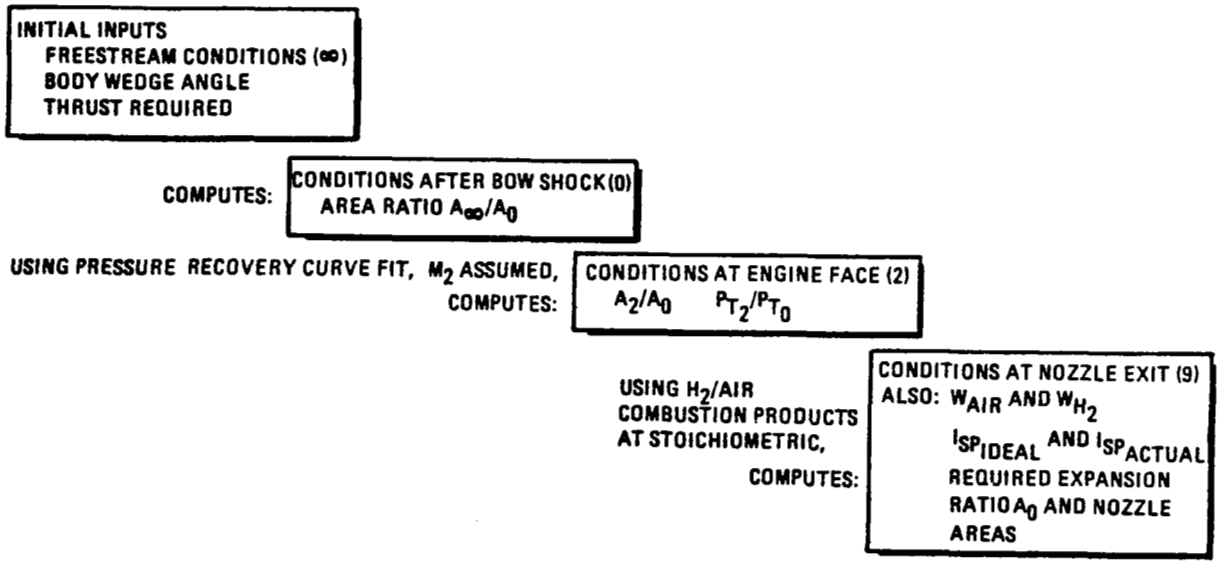

Figure A-9. Computer Program Flow Diagram for Airbreather Propulsion System Sizing

A computer program which has the capability of computing performance of mixed-cycle engines including JP and LH_2 fuel, as well as the air turboexchanger cycle was obtained from the Los Angeles Division of Rockwell (Reference 3). This program was developed under NASA contract in 1966 and is currently used by LAD for calculation of JP-fueled turbojet and turbofan engine data for advanced aircraft.

In order to maximize the payload boosted to orbit, an optimization technique is required to define the proper engine sequencing over the flight trajectory.

A.4 AERODYNAMIC CHARACTERISTICS

The selected wing shape is a supercritical Whitcomb airfoil with a relatively blunt leading edge, flat upper surfaces and cambered trailing edges. The trailing-edge camber and the tri-delta shape minimize translation of the center of pressure throughout the flight Mach number regime. The blunt leading edge offers good subsonic characteristics, but produces relatively high supersonic wave drag; therefore, further shape and refinements are required. The wing has a spanwise thickness distribution of 10 percent at the root, 6 percent near midspan, and 5 percent at the tip, providing a large interior volume for storage of fuel.

Aerodynamic coefficients (C_L, C_D, C.P.) were calculated using the Flexible Unified Distributed Panel program FA-475, which was developed by the LAD Aerodynamic group. Because the governing equation is linear, singular behavior of the linear equation and nonlinearity near M = 1.0 preclude the transonic solutions. Also, the hypersonic solution cannot be calculated with this theory due to the introduction of nonlinear terms. However, aerodynamic coefficients computed at $M_\infty = 5.0$ can be frozen and can be used for hypersonic application. Viscous drag due to the skin friction is not computed by this program. This effect was added in a separate analysis. The resulting aerodynamic coefficients are plotted versus flight Mach number in Figure A-10.

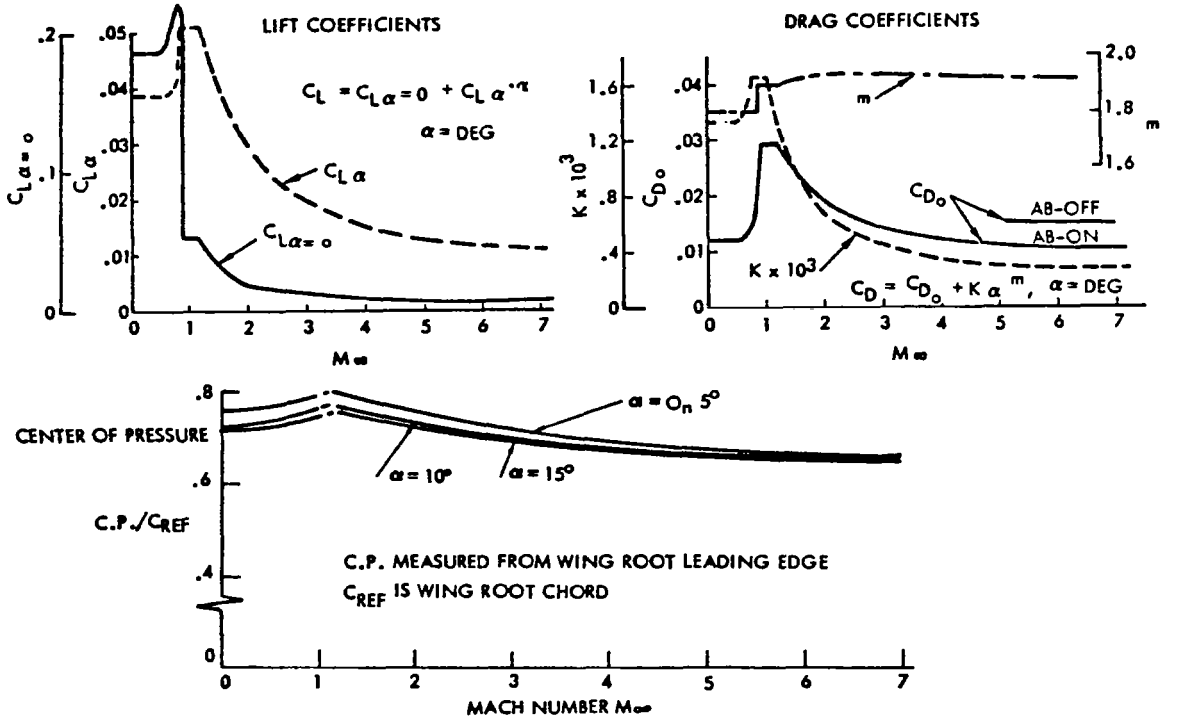

Figure A-10. Aerodynamic Coefficients

Maximum lift/drag and corresponding lift coefficients and angle of attack versus Mach number are given in Figure A-11.

- Subsonic: $(L/D)_{max} \sim 16.0$ at $a \sim 1.0$, $C_L \sim 0.22$
- Supersonic: $(L/D)_{max}$ from 5.4 to 4.0 at $4.5° \leq a \leq 6.2°$
- Hypersonic: For airbreather-OFF, rocket only $(L/D)_{max} \sim 3.4$

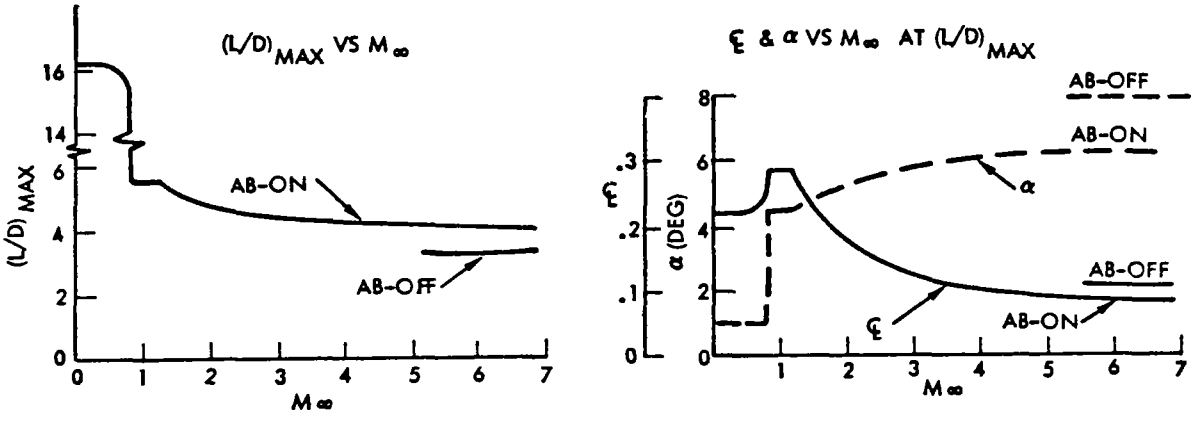

Figure A-11. Maximum Lift/Drag

The wing bending moments are based on the following data:

- Differential pressure distributions computed by the Unified Distributed Panel Program
- X = 10°
- 2 g loading on wing
- GLOW = 4×10^6 lb

Lift force (L_F) and bending moment (BM) at the wing root for the above conditions are shown in the following tabulation.

M_∞	$L_F \times 10^{-6}$ lb	BM x 10^{-6} ft-lb
0.5	4.0	318
0.8	4.0	322
1.2	3.94	334
2.0	3.87	278
3.0	3.8	251
5.0	3.0	185

A.5 FLIGHT MECHANICS

The majority of the ascent performance analysis for the SSTO vehicle concept was accomplished using a recently developed lifting ascent program based on a modified Rutowski Energy Method (Ikawa Method). This technique accurately estimated payload and propellant performance; however, it did not provide a bona fide integrated time history of trajectory state from liftoff to orbit insertion. A second computer program, the Two-Dimensional Trajectory Program (TDTP), was then used to compute the ascent trajectory timeline.

In order to do an end-to-end simulation of the SSTO (i.e., airbreather horizontal takeoff, climb, cruise, turn, airbreather ascent, rocket ascent, coast, and final orbit insertion) with flight optimization including aerodynamic effects, Rockwell acquired the Langley POST computer program (program to optimize simulated trajectories, developed by Martin-Marietta). POST was installed on the CDC system at Rockwell and several launch cases were executed.

The SSTO uses aircraft-type flight from airport takeoff to approximately Mach 6, with a parallel burn transition of airbreather and rocket engines from Mach 6 to 7.2, and rocket-only burn from Mach 7.2 to orbit. Figure A-12 illustrates a nominal trajectory from KSC to 300-nmi earth equatorial orbit. Prime elements of the trajectory are:

- Runway takeoff under high-pass turbofan/airturbo exchanger (ATE)/ ramjet power, with the ramjets acting as supercharged afterburners
- Jettison and parachute recovery of launch gear
- Climb to optimum cruise altitude with turbofan power
- Cruise at optimum altitude, Mach number, and direction vector to earth's equatorial plane, using turbofan power
- Execute a large-radius turn into the equatorial plane with turbofan power
- Climb subsonically at optimum climb angle and velocity to an optimum altitude, using high bypass turbofan/ATE/ramjet (supercharged afterburner) power
- Perform an optimum pitch-over into a nearly constant-energy (shallow γ-angle) dive if necessary, and accelerate through the transonic region to approximately Mach 1.2, using turbofan/ramjet (supercharged afterburner) power
- Execute a long-radius optimum pitch-up to an optimum supersonic climb flight path, using turbofan/ATE/ramjet power
- Climb to approximately 29 km (95 kft) altitude, and 1900 m/s (6200 fps) velocity, at optimum flight path angle and velocity, using proportional fuel-flow throttling from turbofan/ATE/ramjet, or full ramjet, as required to maximize total energy acquired per unit mass of fuel consumed as function of velocity and altitude

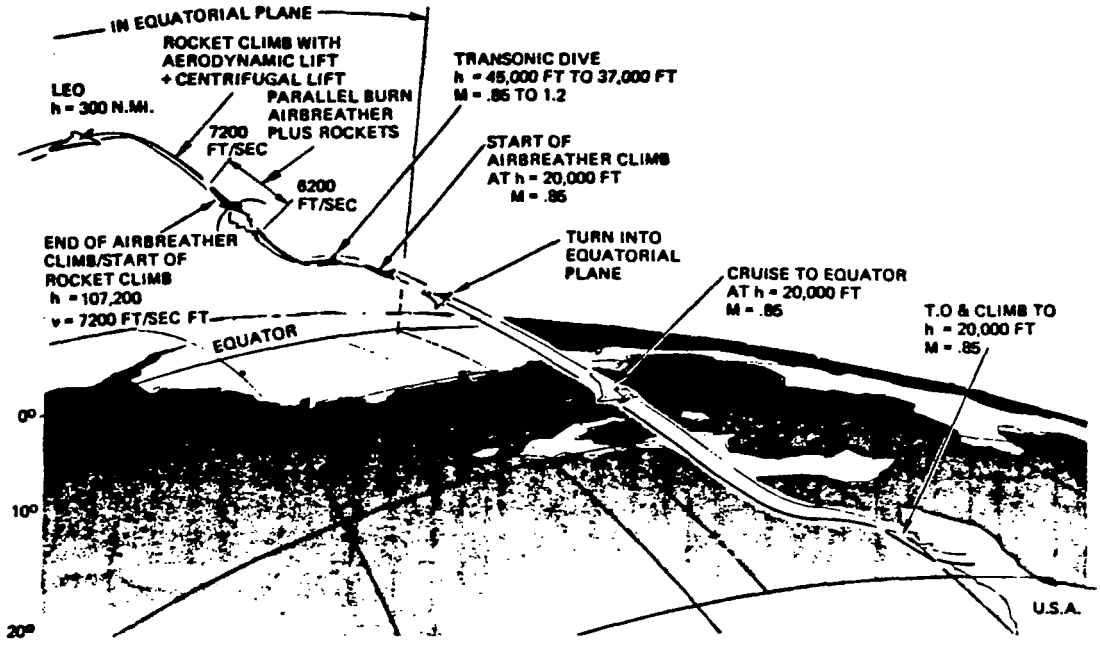

Figure A-12. SSTO Trajectory

- Ignite rocket engines to full required thrust level at 6200 fps and parallel burn to 7200 fps
- Shut down airbreather engines while closing airbreather inlet ramps
- Continue rocket power at full thrust
- Insert into an equatorial elliptical orbit 91×556 km (50×300 nmi) along an optimum lift/drag/thrust flight profile
- Shut down rocket engines and execute a Hohmann transfer to 556 km (300 nmi)
- Circularize Hohmann transfer

The re-entry trajectory is characterized by low gamma (flight path angle) high alpha (angle of attack) similar to Shuttle. The main re-entry trajectory elements are:

- Perform delta velocity (ΔV) maneuver and insert into an equatorial elliptical orbit 91×556 km (50×300 nmi)
- Perform a low-gamma, high-alpha deceleration to approximately Mach 6.0
- Reduce alpha to maximum lift/drag (L/D) for high-velocity glide and cross-range maneuvers to subsonic velocity (approximately Mach 0.85)

- Open inlets and start airbreather engines as required
- Perform powered flight to landing field, land on runway, and taxi to dock

Flyback fuel requirements include approximately 300 nmi subsonic cruise and two landing approach maneuvers (first approach waveoff with flyaround for second approach).

Typical I_{sp} characteristics of AB/rocket engine system are:

- Subsonic range - Linear reduction of I_{sp} from 9700 to 4000 sec at 1200 fps
- Supersonic range - Reduction of I_{sp} from 4000 sec at 1200 fps to 3500 sec at ≈5600 fps (AB)
- Rocket - I_{sp} = 455 sec

The airbreather cruise mode, which results in an economical orbit plane change from the launch site to the equatorial orbit, was analyzed. The estimated fuel requirements to cruise 1000 statute miles down-range for alternate propulsion modes are given below.

V (ft/sec)	Altitude (k-ft)	Δt (sec)	ΔW_F (lb)	Engine
800	20	6600	72,000	Turbofan Jet
6000	85	880	386,000	Ramjet

Although subsonic cruise takes a longer time (110 minutes), the amount of fuel consumed is substantially less when the orbital plane change is accomplished with subsonic cruise at maximum L/D.

A transition maneuver from high-lift configuration to $(L/D)_{max}$ configuration is performed shortly after liftoff (beginning at 3000 ft altitude). The maximum angle of attack of 13 degrees is reduced gradually to 1 degree for subsonic $(L/D)_{max}$ climb configuration.

Velocity and angle of attack vs flight time indicate the time required to reach 300 nmi orbit (not including subsonic cruise leg) varies from 1800 to 2300 sec, depending upon $(W/S)_O$, (T/W), and engine operational mode.

Variation in load factor, altitude, and dynamic pressure with respect to velocity and time during supersonic ascent show a maximum load acceleration less than 2.3 g. Maximum dynamic pressure is 940 psf, which is within load limits. From takeoff to burnout, the ascent profile is quite shallow - with flight path angle ranging between -0.7 and 4.5 degrees.

Ascent and descent trajectories of the SSTO and the Space Shuttle missions are compared in Figure A-13. Because the performance of airbreathing engines and aerodynamic lifting of winged vehicle depend on the high dynamic pressure,

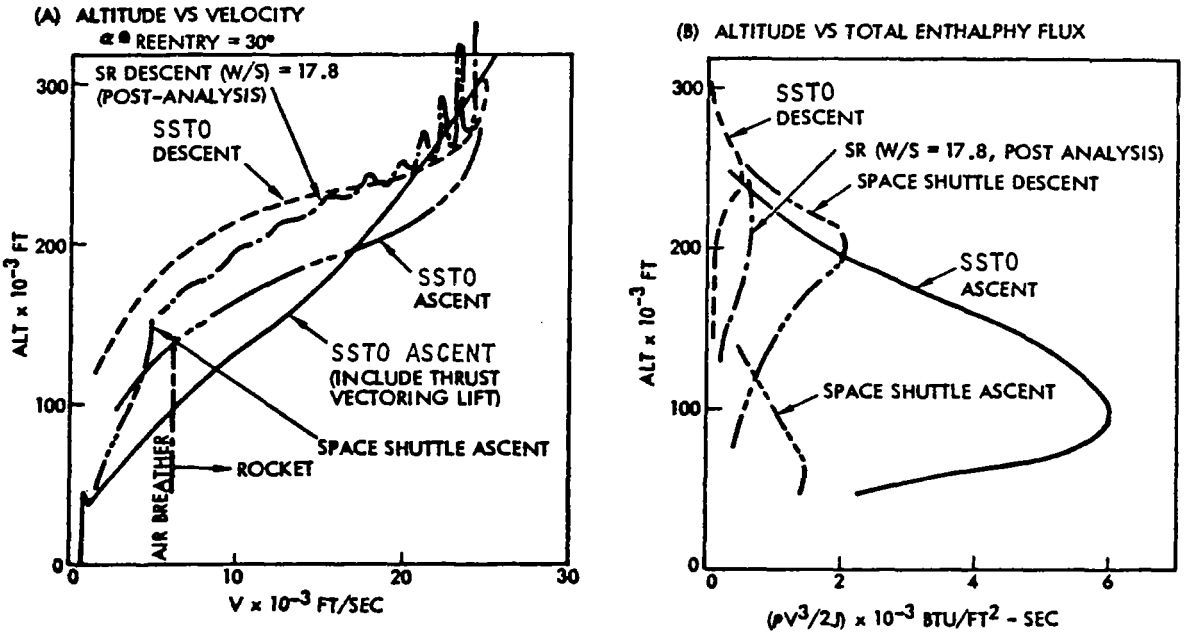

Figure A-13. Ascent and Descent Trajectory Comparisons

the SSTO flies at much lower altitude during the powered climb than the vertical ascent trajectory of the Space Shuttle for a given flight velocity. Light wing loading of the SSTO contributes to the rapid deceleration during deorbit.

The total enthalpy flux histories which indicate the severity of expected aerodynamic heating are shown in Figure A-13. As expected, the aerodynamic heating of ascent trajectory may design the SSTO TPS requirement. The maximum total enthalpy flux of 6000 Btu/ft^2-sec is estimated near the end of airbreather power climb trajectory. Except in the vicinity of vehicle nose, wing leading edge, or structural protuberances, where interference heating may exist, most of the ascent heating is from the frictional flow heating on the relatively smooth flat surface.

The descent heating is mainly produced by the compressive flow on the vehicle windward surface during the high-angle-of-attack re-entry, and is expected to be considerably lower than the Space Shuttle re-entry heating.

Weight in orbit is summarized in Table A-1. The data entries identified by an asterisk are revised reference vehicle data resulting from Rockwell and NASA/MSFC data exchange in May 1978. Calculations reflect additional fuel reserves, performance losses and a 10-percent growth factor. Inert weight in orbit was increased from 694,510 lb to 775,800 lb and airbreather engine thrust of 1.4×10^6 lb constant was revised to reflect increase in airbreather thrust potential shown in Figure A-8.

Table A-1. SSTO Weight in Orbit Summary

ORBIT	GLOW $W_o \times 10^6$ LB	ROCKET I_{SP} = 455. SEC (SHUTTLE VALUES)				ROCKET I_{SP} = 468 SEC (LaRC VALUES)	
		ENERGY METHOD		POST ANALYSIS		ENERGY METHOD	
		W_f (LB)	PAYLOAD (LB)	W_f (LB)	PAYLOAD (LB)	W_f (LB)	PAYLOAD (LB)
EQUATORIAL ORBIT CRUISE FROM KSC	4.31 4.31 (P.B) 4.62 (P.B) 5.00 (P.B)	787,400. 801,700. 845,800. 895,300.	92,890. 107,190. 151,290. 200,790.	790,000.	95,490.	832,800.	138,290.
INCLINED ORBIT KSC DUE EAST	4.31 4.31 (P.B) 4.62 (P.B) *5.00 (PB)	864,500. 882,600 925,100.	169,990. 188,090. 230,590.	849,000. *972,400	154,490 *196,580	897,000. 917,300.	202,490. 222,790.

- DATA FOR 300 N MI. ORBITAL INSERTION
- REFERENCE WING AREA (S_{REF}) = 40,900. SQ. FT.
- WEIGHT IN ORBIT (EXCLUDING PAYLOAD) = 694,510. LB * = 775,800 LB
- LAUNCH FROM KSC
- PB = PARALLEL BURN
- AIRBREATHER
  - THRUST = 1.4×10^6 LB.
  - I_{SP} = VARIABLE
  - VELOCITY = $0 \leq V \leq 6200$ FT/SEC
- ROCKET
  - THRUST = 3.2×10^6 LB
  - I_{SP} = SEE CHART
  - VELOCITY = $6200 \leq V \leq V_{ORBIT}$ FT/SEC

A.6 AERODYNAMIC AND STRUCTURAL HEATING

Preliminary aerodynamic heating evaluation of the SSTO configuration was performed for several wing spanwise stations and the fuselage centerline.

For the wing lower surfaces, heating rates were computed including the chordwise variation of local flow properties. Effects of leading edge shock and angle of attack were included in the local flow property evaluation. Leading edge stagnation heating rates were based on the flow conditions normal to the leading edge neglecting cross-flow effects. All computations were performed using ideal gas thermodynamic properties.

Wing upper-surface heating rates were computed using free-stream flow properties, i.e., neglecting chordwise variations of flow properties. Heating rates were computed for several prescribed wall temperatures as well as the reradiation equilibrium wall temperature condition. Transition from laminar to turbulent flow was taken into account in the computations. Wing/body and inlet interference heating effects were not included in this preliminary analysis. The analysis was limited to the ascent trajectory, since the descent trajectory is thermodynamically less severe.

These parametrically generated aerodynamic heating rate data were used for thermal analysis of the various candidate insulation systems. Radiation equilibrium temperatures for emissivity, $\varepsilon = 0.85$, are based on:

- Leading edge stagnation heating rates peak at M = 16.4, alt = 196,000 ft
- Upper wing surface uniform static pressure assumed, temperatures peak at M = 6.4, alt = 86,500 ft
- Lower wing surface heating rates and temperatures peak at M = 7.9, alt = 116,000 ft
- Local flow property variation, angle of attack, and leading-edge shock effects are included
- Inlet interference effects were not included

Isotherms of the peak surface temperatures for upper and lower surfaces (excluding engine inlet interference effects) for the SSTO and Orbiter are shown in Figure A-14. Leading edge and upper wing surface temperatures have similar profiles. The SSTO lower-surface temperatures are from 400°F to 600°F lower than the orbiter due to lower re-entry wing loading (23 versus 67 psf).

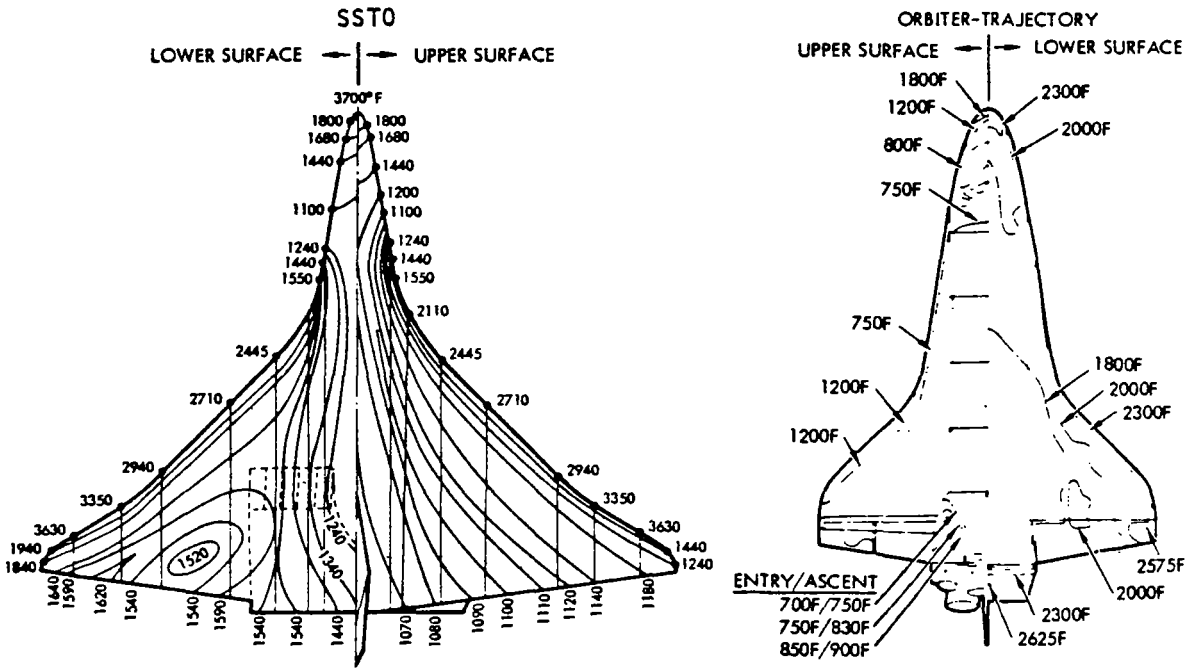

Figure A-14. Isotherms of Peak Surface Temperatures During Ascent

Structural heating analyses include: (a) typical variations of heat leak rate (BTU/ft^2-hr) and total heat flux (BTU/ft^2) as a function of HRSI tile thickness for typical LH_2 upper and lower wing tank surface locations; (b) variation of bondline temperatures versus tile maximum temperature to thickness ratio for RSI tile insulation, including bondline temperatures for the dry, wingtip ullage tank, the wetted lower surface of the LH_2 tank, and the dry upper surface

of the LH_2 tank; and (c) typical thermal response as a function of launch trajectory exposure time of the insulation system.

Figure A-15 shows HRSI tile thickness profiles for bondline temperatures of 350°F. Preliminary data indicate that the titanium aluminide system described in the TPS section of this report may be lighter than the RSI tile for the SSTO TPS system due to the low average temperature (1000°F to 1600°F) profiles occurring over 80 and 85 percent of the vehicle exterior surface.

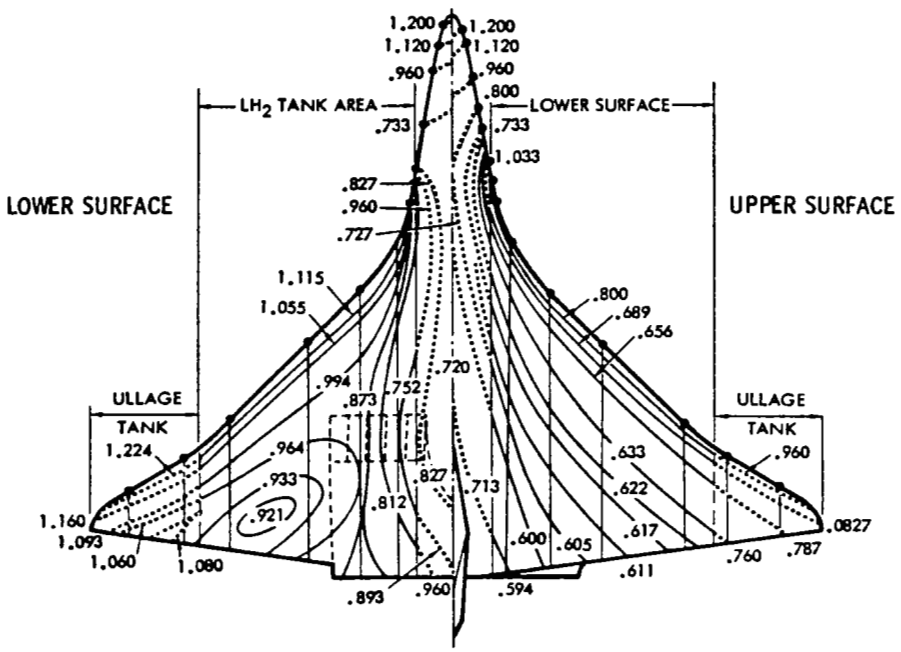

Figure A-15. HRSI Tile Thickness Contours for 350°F Bondline Temperature

A.7 THERMAL PROTECTION SYSTEM

Ceramic coated RSI tile,used on Shuttle, and metallic truss core sandwich structure, developed for the B-1 bomber, were investigated as potential thermal protection systems for the SSTO, Figure A-5.

The radiative surface panel consists of a truss core sandwich structure fabricated by superplastic/diffusion bonding process. For temperatures up to 1500/1600°F, the concept utilizes an alloy based on the titanium-aluminum systems which show promise for high-temperature applications currently being developed by the Air Force. For temperatures higher than 1500/1600°F, it is anticipated that an alloy will be available from the dispersion-strengthened superalloys currently being developed for use in gas turbine engines. Flexible supports are designed to accommodate longitudinal thermal expansion while retaining sufficient stiffness to transmit surface pressure loads to the primary structure. Also prominent in metallic TPS designs are expansion joints which must absorb longitudinal thermal growth of the radiative surface, and simultaneuously prevent the ingress of hot boundary layer gases to the panel interior.

The insulation consists of flexible thermal blankets, often encapsulated in foil material to prevent moisture absorption. The insulation protects the primary load-carrying structure from the high external temperature.

During the past two years, Rockwell and Pratt and Whitney Aircraft have participated in an Air Force Materials Laboratory sponsored program, F33615-75-C-1167, directed toward the exploitation of Ti_3Al base alloy systems. The titanium aluminide intermetallic compounds based on the compositions Ti_3Al (α_2) and TiAl (γ) which form the binary Ti-Al alloys have been shown to have attractive elevated-temperature strength and high modulus/density ratios.

Titanium hardware of complex configurations have been developed, utilizing a process which combines superplastic forming and diffusion bonding (SPF/DB). This Rockwell proprietary process has profound implications for titanium fabrication technology, per se. In addition, the unprecedented low-cost hardware it generates promises to revolutionize the design of airframe structure. The versatile nature of the process may be shown by the nature of the complex deep-drawn structure and sandwich structure with various core configurations which have been fabricated. This manufacturing method and the design freedom it affords offer a solution to the high cost of aircraft structure. Manufacturing feasibility and cost and weight savings potential of these processes have been established through both IR&D efforts at Rockwell and Air Force contracts. These structures may be used for engine cowling, landing gear doors, etc., in addition to providing major TPS components.

Unit masses of the SSTO TPS concept, state-of-the-art TPS hardware and advanced thermal-structural designs are compared with the unit mass of the orbiter RSI in Figure A-16. The unit mass of the RSI includes the tiles, the strain isolator pad, and bonding material. The hashed region shown for the RSI mass is indicative of insulation thickness variations necessary to maintain mold line over the bottom surface of the orbiter. The RSI is required to prevent the primary structure temperature from exceeding 350°F. The unit masses of the metallic TPS are plotted at their corresponding maximum use temperatures. The advanced designs are seen to be competitive with the directly bonded RSI.

A.8 STRUCTURAL ANALYSIS

The multi-cell wing tanks provide a structure which is capable of sustaining pressure while, at the same time, reacting aerodynamic loads. The tanks are sized based on ullage pressures of 32-34 psia (LH_2) and 22-22 psia (LOX). Maximum wing bending occurs at about Mach 1.2. The LH_2 and LOX wing tanks are the major load path for reacting these loads. The wing also supports the air-breather engine system.

The primary wing attachment is to the cargo bay structure. The cargo bay aft section, in turn, is connected to the LH_2 tank. The LH_2 interconnects the cargo bay, aft portions of the wing, the vertical surface, and the rocket engine thrust structure.

An ultimate factor of safety of 1.50 was used in the analysis. The prime driver in the structural sizing of the multi-cell wing tanks is the bending moment resulting from air loads at Mach 1.2. The net bending moment on the

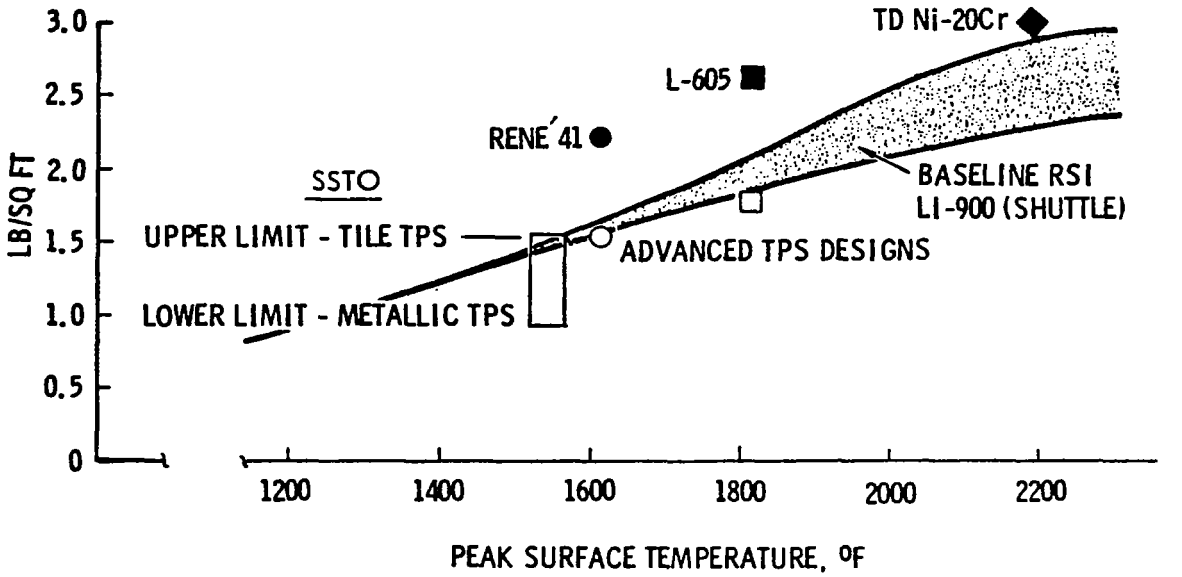

Figure A-16. Unit Mass of TPS Designs

wing is the difference between the lift moment and the relieving moment due to LOX remaining in the wing. Trades were performed to determine the structural wing weights required to sustain these bending moments plus internal pressure. An intermediate location was chosen for LOX propellant where lift moment ~2 times relieving moment. Locating LOX outboard results in a lower net flight bending moment, but the critical design condition then becomes prelaunch under full propellant loading. To sustain this prelaunch bending moment, the wing weight would be in excess of 200,000 lb.

The wing LH_2 tank was designed to sustain the loads from both internal pressure and wing bending. Al 2219-T87 was chosen for the tank material on the basis of high strength at cryogenic temperatures, fracture toughness, and weldability. Loads resulting from wing bending moments are dominant in determining membrane thickness, which is based on a maximum tank ullage pressure of 34 psia, and an ultimate factor of safety of 1.50. Figure A-17 shows material thickness versus wing station due to pressure and wing bending. The column showing bending only relates to wing-bending contribution, not an unpressurized wing design.

The fuselage LH_2 tank is the primary load path for reacting total vehicle mass inertias during the maximum acceleration condition (3.0 g). Approximately 27 percent of the propellant remains at that time. The tank has a twin-cone "Siamese" configuration which is required in order to fit in the fuselage at maximum propellant volume. The forward end of the tank is cylindrical, while the aft end is closed out with a double modified ellipsoidal shell. The bulkheads react the internal pressures while the sidewall carries pressure and axial compression loads. The bulkheads are monocoque construction while the sidewall is an integral skin-stringer with ring frames construction. Tank

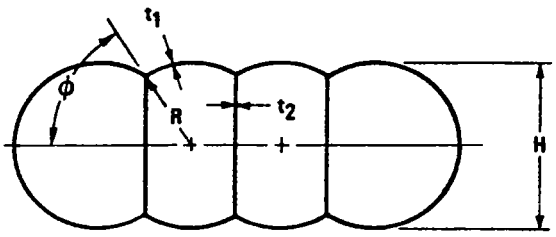

STA* (FT)	H_{NOM} (IN.)	PRESSURE REQUIREMENT $t_1 = t_2$** (IN.)	BENDING ONLY t_1 (IN.)	BENDING + PRESSURE t_1 (IN.)
10.9	240	0.066	0.021	0.087
23.0	146	0.040	0.076	0.116
54.0	110	0.031	0.092	0.123
107.0	48	0.014	0.120	0.134

*DISTANCE FROM VEHICLE ℄
**FOR ∅ = 60 DEG ONLY

Figure A-17. Material Thickness Versus Wing Station

configuration and bulkhead membrane and sidewall "smeared" thickness requirements to sustain the internal pressure and axial compression loads have been determined. The structural design of all cryo tanks is based on cryogenic temperature material properties and allowables.

A.9 MASS PROPERTIES

SSTO mass properties are dominated by the tri-delta wing structure, the thermal protection system and the airbreather and rocket propulsion system. The initial reference vehicle data, shown in Table A-2, were generated by Rockwell during the period of December 1977 - January 1978. These data were reviewed by NASA MSFC/LaRC during February and March 1978, resulting in two extremes of mass estimates. A reassessment by Rockwell during May produced the final reference vehicle data. The data presented in this report are considered to be reasonably achievable targets. The technology items coded on Figure A-1 require study in greater depth and degree of sophistication to confirm SSTO mass property data.

Table A-2. SSTO Weight Summary

ITEM DESCRIPTION	ROCKWELL	MSFC		ROCKWELL
	INITIAL REFERENCE VEHICLE	NORMAL TECHNOLOGY	ACCELER TECHNOLOGY	FINAL REFERENCE VEHICLE
AIRFRAME, AEROSURFACES, TANKS AND TPS	367,000	458,000	249,000	370,000
LANDING GEAR	27,700	53,000	39,000	27,700
ROCKET PROPULSION	63,700	40,000	40,000	71,700
AIRBREATHER PROPULSION	148,000	200,000	148,000	140,000
RCS PROPULSION	4,000	16,000	11,000	10,000
OMS PROPULSION	1,200	9,000	7,000	5,000
OTHER SYSTEMS	35,500	41,000	22,000	37,800
SUBTOTAL	647,100	817,000	516,000	662,200
10% GROWTH		81,700	51,600	66,220
TOTAL INERT WEIGHT (DRY WEIGHT)	647,100	898,700	567,600	728,420
USEFUL LOAD (FLUIDS, RESERVES, ETC.)	47,400	—	—	47,400
INERT WEIGHT & USEFUL LOAD	694,500	—	—	775,820
PAYLOAD WEIGHT	107,200			196,580
ORBITAL INSERTION WEIGHT	801,700	—	—	972,400
PROPELLANT ASCENT	3,438,080			4,027,600
GLOW (POST-JETTISON LAUNCH GEAR)	4,239,780	—	—	5,000,000

300 NMI EQUATORIAL ORBIT
NOTE: THIS VEHICLE HAS 51,000 CU FT EXCESS PROPELLANT TANK VOLUME SEE WEIGHT IN ORBIT SUMMARY

300 NMI, 28.5° INCLINED ORBIT

REFERENCES

1. *Estimated Performance of a Mach 8.0 Hydrogen Fueled Turbofan Ramjet,* Pratt and Whitney Aircraft Report STFRV-230A (January 1965)

2. *Air-Turborocket Application Study,* Aerojet General Corporation (December 1964)

3. *Final Report and Users Manual for the Hypersonic Airbreathing Propulsion Computer Program, NASA Contract NAS2-2985,* North American Aviation Reports NA66-479 and NA66-530 (May 1966)

4. *Airbreathing Engine/Rocket Trajectory Optimization Study,* Virgil K. Smith, University of Alabama (August 1978)

5. *Feasibility Study of Reusable Aerodynamic Space Vehicle,* SAMSO-TR-76-223, Boeing Aerospace Company (November 1976)